A Voltage Modulated Direct Power Control of the Doubly Fed Induction Generator

Gao, Shuning; Zhao, Haoran; Gui, Yonghao; Zhang, Zhenbin; Wu, Qiuwei

Published in:
2019 IEEE Power & Energy Society General Meeting (PESGM)

DOI (link to publication from Publisher):
10.1109/PESGM40551.2019.8973524

Publication date:
2019

Document Version
Accepted author manuscript, peer reviewed version

A Voltage Modulated Direct Power Control of the Doubly Fed Induction Generator

Shuning Gao[1], Haoran Zhao[2], Yonghao Gui[3], Zhenbing Zhang[2], Qiuwei Wu[4]
[1]School of Electrical Engineering, Shandong University, Ji'nan 250061, China.
[2]Key Laboratory of Power System Intelligent Dispatch and Control of Ministry of Education, Shandong University, Ji'nan 250061, China.
[3]Automation & Control Section, Department of Electronic Systems, Aalborg University, Aalborg, Denmark .
[4]Department of Electrical Engineering, Technical University of Denmark, Lyngby, Denmark.
(email:gaosn@mail.sdu.edu.cn, hzhao@sdu.edu.cn, yg@es.aau.dk, zbz@sdu.edu.cn, qw@elektro.dtu.dk)

***Abstract*—In this paper, a Voltage Modulated Direct Power Control (VM-DPC) for doubly fed induction generator is proposed. The suggested method is implemented in the rotor reference frame, so that the phase-lock loop can be removed and relevant potential instability can be eliminated. The main advantage is that the proposed method has a relative simple structure compare to conventional Look-Up Table (LUT) DPC and sliding mode control (SMC), besides, it not only guarantees an enhanced transient performance but also keeps the steady-state harmonic spectra at the same level as voltage-oriented strategy. Finally, a simulation based on MATLAB/Simulink is provided to validate the performance of proposed VM-DPC strategy.**

***Index Terms*—Control of doubly fed induction generator, direct power control (DPC), voltage modulated**

I. INTRODUCTION

Nowadays, Doubly Fed Induction Generators (DFIGs) are widely used in modern wind power generation systems because of its multiple advantages such as flexible active and reactive power control capability, variable speed operation, low-converter cost and high reliability. The DFIG wind-turbine consists of a back-to-back converter and a wound rotor induction generator, the stator windings of which are directly connected to Point of Common Connection (PCC) of the grid [1].

Traditional control of back-to-back converters in DFIGs is usually designed based on stator voltage-oriented or stator flux oriented vector control, which requires a decoupled proportional-integral (PI) controller to control d-q axes currents seperately [2]. However, the transient response of traditional voltage oriented control (VOC) is often unsatisfactory due to the slow dynamics of the PLL which has been widely adopted in the signal decoupling process [3].

Direct power control (DPC) technique is proposed and proved to have many advantages in recent years such as simple implemented, fast power responses and parameter robustness thus has been widely in DFIG integrated power system [2]–[12]. The switching signal can be generated by look-up table (LUT) or Space Vector Modulation (SVM) [13].

One main problem of LUT based DPC is that the converter switching frequency varies with operating conditions and torque/flux hysteresis controllers' bandwidth, which significantly complicates power circuit designs and results in obvious torque pulsations [3]. Thus predictive direct control techniques are emerging as an alternative solution to the main drawbacks of traditional LUT based method caused by various switching frequency. [12], [14]. An improved coordinate DPC for the DFIG using SVM under unbalanced grid conditions is proposed in [6]. The sliding mode control direct power control (SMC-DPC) techniques for DFIG generation system were presented in many recent papers [3], [8], [15], which can improve transient performance of generation system. Yet the fast switching in SMC-DPC may generate unexpected chattering. To eliminate that problem, a boundary layer around the sliding surface is proposed in [3]. Nonetheless, the controller structures mentioned above are relatively complex and not easy to be used in practice.

Recently, a grid voltage modulated-DPC (GVM-DPC) is proposed for grid connected voltage source converters, where the GVM-DPC overcomes the steady-state performance of the DPC, which is the main disadvantage [16], [17]. Moreover, the GVM-DPC converts the system into a linear time-invariant one, which could be analyzed based on various control techniques [18], [19].

In this paper, a simple direct power control combined with VM-DPC is proposed to achieve better operation of DFIG. Design of the controller takes advantage of a simple yet robust control strategy proposed in [18]. The strategy only decoupled voltage and current component in rotor reference frame (DQ) therefore the phase signal of stator voltage is unnecessary. The rest of this paper is organized as follows. In section II, the mathematical model of DFIG in rotor (DQ) reference frame is presented. Section III describes the controller design and Section IV presents the simulation result which shows comparison between the proposed control strategy and traditional vector oriented controller (VOC). Finally, the conclusions are given in Section V.

This work was supported by the National Key R&D Program of China(2018YFB0904004) and in part by Natural Science Foundation of China under Grants 51707106 *(Corresponding author: Haoran Zhao).*

II. Mathematical model of DFIG

To understand how the stator active and reactive power can be directly controlled by modifying the rotor voltage space vector in rotor reference frame (DQ), a mathematical model of DFIG is established in this section.

By referring the space vector in stator reference frame (dq) to the rotor reference frame (DQ), the DQ model of DFIG can be obtained. The stator side and rotor side voltage can be represented in DQ reference frame as follows,

$$\boldsymbol{v}_{\mathrm{s}}{}^{\mathrm{r}} = R_{\mathrm{s}}\boldsymbol{i}_{\mathrm{s}}{}^{\mathrm{r}} + \frac{\mathrm{d}\boldsymbol{\psi}_{\mathrm{s}}{}^{\mathrm{r}}}{\mathrm{d}t} + j\omega_{\mathrm{m}}\boldsymbol{\psi}_{\mathrm{s}}{}^{\mathrm{r}}, \tag{1}$$

$$\boldsymbol{v}_{\mathrm{r}}^{\mathrm{r}} = R_{\mathrm{r}}\boldsymbol{i}_{\mathrm{r}}^{\mathrm{r}} + \frac{\mathrm{d}\boldsymbol{\psi}_{\mathrm{r}}^{\mathrm{r}}}{\mathrm{d}t}, \tag{2}$$

where ω_{m} is the angular frequency of rotor, R_{s} and R_{r} represent stator and rotor resistances. In (1) and (2), the superscripts $'\mathrm{r}'$ indicate the rotor reference frames. The subscripts $'\mathrm{s}'$ and $'\mathrm{r}'$ indicate the stator and rotor side, respectively. Therefore, $\boldsymbol{v}_{\mathrm{s}}{}^{\mathrm{r}}$ and $\boldsymbol{v}_{\mathrm{r}}^{\mathrm{r}}$ represent the stator and rotor voltage space vector. $\boldsymbol{i}_{\mathrm{s}}{}^{\mathrm{r}}$ and $\boldsymbol{i}_{\mathrm{r}}^{\mathrm{r}}$ represent stator and rotor current space vector. $\boldsymbol{\psi}_{\mathrm{s}}{}^{\mathrm{r}}$ and $\boldsymbol{\psi}_{\mathrm{r}}^{\mathrm{r}}$ represent the stator flux space vector, respectively. The space vector mentioned above can be expressed in DQ reference frame as: $\boldsymbol{v}_{\mathrm{s}}^{\mathrm{r}} = v_{\mathrm{sD}} + jv_{\mathrm{sQ}}$,$\boldsymbol{v}_{\mathrm{r}}^{\mathrm{r}} = v_{\mathrm{rD}} + jv_{\mathrm{rQ}}$, $\boldsymbol{\psi}_{\mathrm{s}}^{\mathrm{r}} = \psi_{\mathrm{sD}} + j\psi_{\mathrm{sQ}}$,$\boldsymbol{\psi}_{\mathrm{r}}^{\mathrm{r}} = \psi_{\mathrm{rD}} + j\psi_{\mathrm{rQ}}$. The relationship between stator reference frame ($\alpha\beta$) and rotor reference frame (DQ) is shown in Fig. 1. The flux linkage and current relation at both stator and rotor side can be expressed as follows,

$$\boldsymbol{\psi}_{\mathrm{s}}^{\mathrm{r}} = L_{\mathrm{s}}\boldsymbol{i}_{\mathrm{s}}^{\mathrm{r}} + L_{\mathrm{m}}\boldsymbol{i}_{\mathrm{r}}^{\mathrm{r}}, \tag{3}$$

$$\boldsymbol{\psi}_{\mathrm{r}}^{\mathrm{r}} = L_{\mathrm{r}}\boldsymbol{i}_{\mathrm{r}}^{\mathrm{r}} + L_{\mathrm{m}}\boldsymbol{i}_{\mathrm{s}}^{\mathrm{r}}, \tag{4}$$

where L_{s} and L_{r} are total self-inductances of stator and rotor winding, and L_{m} is mutual inductance. The equivalent circuit of DFIG in rotor reference frame (DQ) is shown in Fig. 2.

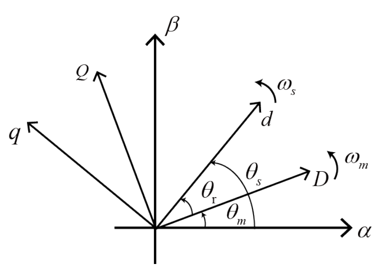

Fig. 1. Relationship between ($\alpha\beta$), dq, DQ reference frames.

Substituting (3) and (4) into (1) and (2), the voltage can be expressed as,

$$\boldsymbol{v}_{\mathrm{s}}^{\mathrm{r}} = R_{\mathrm{s}}\boldsymbol{i}_{\mathrm{s}}^{\mathrm{r}} + \frac{\mathrm{d}}{\mathrm{d}t}(L_{\mathrm{s}}\boldsymbol{i}_{\mathrm{s}}^{\mathrm{r}} + L_{\mathrm{m}}\boldsymbol{i}_{\mathrm{r}}^{\mathrm{r}}) + j\omega_{\mathrm{m}}(L_{\mathrm{s}}\boldsymbol{i}_{\mathrm{s}}^{\mathrm{r}} + L_{\mathrm{m}}\boldsymbol{i}_{\mathrm{r}}^{\mathrm{r}}), \tag{5}$$

$$\boldsymbol{v}_{\mathrm{r}}^{\mathrm{r}} = R_{\mathrm{r}}\boldsymbol{i}_{\mathrm{r}}^{\mathrm{r}} + \frac{\mathrm{d}}{\mathrm{d}t}(L_{\mathrm{r}}\boldsymbol{i}_{\mathrm{r}}^{\mathrm{r}} + L_{\mathrm{m}}\boldsymbol{i}_{\mathrm{s}}^{\mathrm{r}}). \tag{6}$$

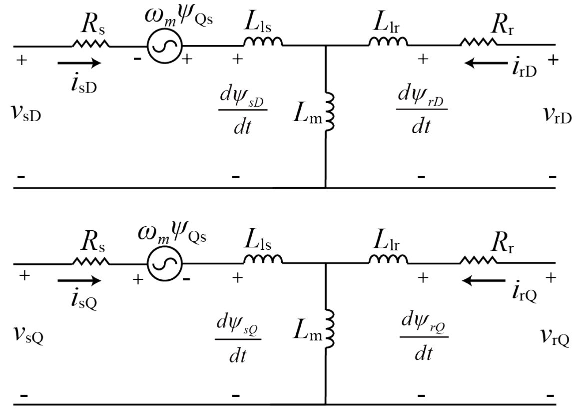

Fig. 2. Equivalent circuit of a DFIG in the rotor (DQ) reference frame.

By manipulating (5) and (6) to eliminate term $d\boldsymbol{i}_{\mathrm{r}}^{\mathrm{r}}/dt$, the relationship between stator current and stator/rotor voltage yields as follows,

$$\begin{aligned}\boldsymbol{v}_{\mathrm{s}}^{\mathrm{r}} - \frac{L_{\mathrm{m}}}{L_{\mathrm{r}}}\boldsymbol{v}_{\mathrm{r}}^{\mathrm{r}} =& R_{\mathrm{s}}\boldsymbol{i}_{\mathrm{s}}^{\mathrm{r}} + L_{\mathrm{s}}\frac{\mathrm{d}\boldsymbol{i}_{\mathrm{s}}^{\mathrm{r}}}{\mathrm{d}t} + j\omega_{\mathrm{m}}L_{\mathrm{s}}\boldsymbol{i}_{\mathrm{s}}^{\mathrm{r}} + j\omega_{\mathrm{m}}L_{\mathrm{m}}\boldsymbol{i}_{\mathrm{r}}^{\mathrm{r}} \\ &- \frac{R_{\mathrm{r}}L_{\mathrm{m}}}{L_{\mathrm{r}}}\boldsymbol{i}_{\mathrm{r}}^{\mathrm{r}} - \frac{{L_{\mathrm{m}}}^2}{L_{\mathrm{r}}}\frac{\mathrm{d}\boldsymbol{i}_{\mathrm{s}}^{\mathrm{r}}}{\mathrm{d}t}.\end{aligned} \tag{7}$$

Based on (7), the instantaneous variation of stator current can be expressed in the DQ reference frame as follows:

$$\begin{cases}\frac{\mathrm{d}i_{\mathrm{sD}}}{\mathrm{d}t} = \frac{1}{\sigma L_{\mathrm{s}}}(v_{\mathrm{sD}} - \frac{L_{\mathrm{m}}}{L_{\mathrm{r}}}v_{\mathrm{rD}} - R_{\mathrm{s}}i_{\mathrm{sD}} + \frac{R_{\mathrm{r}}L_{\mathrm{m}}}{L_{\mathrm{r}}}i_{\mathrm{rD}} \\ \quad + \omega_{\mathrm{m}}L_{\mathrm{s}}i_{\mathrm{sQ}} + \omega_{\mathrm{m}}L_{\mathrm{m}}i_{\mathrm{rQ}} \\ \frac{\mathrm{d}i_{\mathrm{sQ}}}{dt} = \frac{1}{\sigma L_{\mathrm{s}}}(v_{\mathrm{sQ}} - \frac{L_{\mathrm{m}}}{L_{\mathrm{r}}}v_{\mathrm{rQ}} - R_{\mathrm{s}}i_{\mathrm{sQ}} \\ \quad + \frac{R_{\mathrm{r}}L_{\mathrm{m}}}{L_{\mathrm{r}}}i_{\mathrm{rQ}} - \omega_{\mathrm{m}}L_{\mathrm{s}}i_{\mathrm{sD}} - \omega_{\mathrm{m}}L_{\mathrm{m}}i_{\mathrm{rD}}\end{cases}, \tag{8}$$

where $\sigma = 1 - \frac{L_{\mathrm{m}}^2}{L_{\mathrm{s}}L_{\mathrm{r}}}$. The active and reactive power of stator side can be expressed as

$$P_{\mathrm{s}} + jQ_{\mathrm{s}} = \frac{3}{2}v_{\mathrm{s}}^{\mathrm{r}} \cdot i_{\mathrm{s}}^{\mathrm{r}*}. \tag{9}$$

Differentiating (9) results in instantaneous variations of stator active and reactive powers as

$$\begin{cases}\frac{\mathrm{d}P_{\mathrm{s}}}{\mathrm{d}t} = \frac{3}{2}(\frac{\mathrm{d}v_{\mathrm{sD}}}{\mathrm{d}t}i_{\mathrm{sD}} + \frac{\mathrm{d}i_{\mathrm{sD}}}{\mathrm{d}t}v_{\mathrm{sD}} + \frac{\mathrm{d}v_{\mathrm{sQ}}}{\mathrm{d}t}i_{\mathrm{sQ}} + \frac{\mathrm{d}i_{\mathrm{sQ}}}{\mathrm{d}t}v_{\mathrm{sQ}}) \\ \frac{\mathrm{d}Q_{\mathrm{s}}}{\mathrm{d}t} = \frac{3}{2}(\frac{\mathrm{d}v_{\mathrm{sQ}}}{\mathrm{d}t}i_{\mathrm{sD}} + \frac{\mathrm{d}i_{\mathrm{sD}}}{\mathrm{d}t}v_{\mathrm{sQ}} - \frac{\mathrm{d}v_{\mathrm{sD}}}{\mathrm{d}t}i_{\mathrm{sQ}} - \frac{\mathrm{d}i_{\mathrm{sQ}}}{\mathrm{d}t}v_{\mathrm{sD}}).\end{cases} \tag{10}$$

As expressed in (10), the instantaneous network voltage variation is required, considering an ideal network and the network voltage angular frequency ω_1 is equal to stator synchronous frequency ω_s: $\omega_1 = \omega_s$, i.e.,

$$\begin{cases} v_{\mathrm{sD}} = |v_{\mathrm{s}}|\cos[(\omega_{\mathrm{s}} - \omega_{\mathrm{m}})\mathrm{t} + \theta_0] \\ v_{\mathrm{sQ}} = |v_{\mathrm{s}}|\sin[(\omega_{\mathrm{s}} - \omega_{\mathrm{m}})\mathrm{t} + \theta_0]. \end{cases} \tag{11}$$

Thus, the instantaneous network voltage variation can be obtained as,

$$\begin{cases} \dfrac{\mathrm{d}v_{\mathrm{sD}}}{\mathrm{d}t} = -\omega_{\mathrm{r}} v_{\mathrm{sQ}} \\ \dfrac{\mathrm{d}v_{\mathrm{sQ}}}{\mathrm{d}t} = \omega_{\mathrm{r}} v_{\mathrm{sD}}. \end{cases} \tag{12}$$

Where ω_{r} is the angular frequency of the voltages and currents of the rotor windings which can be expressed as: $\omega_{\mathrm{r}} = \omega_s - \omega_{\mathrm{m}}$. By manipulating (8), (10) and (12), the dynamics of instantaneous active and reactive power yield,

$$\begin{aligned} \frac{\mathrm{d}P_{\mathrm{s}}}{\mathrm{d}t} =& -(\frac{\omega_{\mathrm{m}}}{\sigma} + \omega_{\mathrm{r}})Q_{\mathrm{s}} - \frac{R_{\mathrm{s}}}{\sigma L_{\mathrm{s}}} P_{\mathrm{s}} + \frac{3}{2\sigma L_{\mathrm{s}}}[|v_{\mathrm{s}}|^2 \\ & - \frac{L_{\mathrm{m}}}{L_{\mathrm{r}}}(v_{\mathrm{rD}} v_{\mathrm{sD}} + v_{\mathrm{rQ}} v_{\mathrm{sQ}}) + \frac{R_{\mathrm{r}} L_{\mathrm{m}}}{L_{\mathrm{r}}}(v_{\mathrm{sD}} i_{\mathrm{rD}} + v_{\mathrm{sQ}} i_{\mathrm{rQ}}) \\ & + \omega_{\mathrm{m}} L_{\mathrm{m}}(v_{\mathrm{sD}} i_{\mathrm{rQ}} - v_{\mathrm{sQ}} i_{\mathrm{rD}})], \end{aligned} \tag{13}$$

$$\begin{aligned} \frac{\mathrm{d}Q_{\mathrm{s}}}{\mathrm{d}t} =& (\frac{\omega_{\mathrm{m}}}{\sigma} + \omega_{\mathrm{r}})P_{\mathrm{s}} - \frac{R_{\mathrm{s}}}{\sigma L_{\mathrm{s}}} Q_{\mathrm{s}} + \frac{3}{2\sigma L_{\mathrm{s}}}[-\frac{L_{\mathrm{m}}}{L_{\mathrm{r}}}(v_{\mathrm{rD}} v_{\mathrm{sQ}} - \\ & v_{\mathrm{rQ}} v_{\mathrm{sD}}) + \frac{R_{\mathrm{r}} L_{\mathrm{m}}}{L_{\mathrm{r}}}(v_{\mathrm{sQ}} i_{\mathrm{rD}} - v_{\mathrm{sD}} i_{\mathrm{rQ}}) \\ & + \omega_{\mathrm{m}} L_{\mathrm{m}}(v_{\mathrm{sQ}} i_{\mathrm{rQ}} + v_{\mathrm{sD}} i_{\mathrm{rD}})]. \end{aligned} \tag{14}$$

III. Voltage modulated DPC design for RSC

Let us define voltage modulated regulation (VMR) inputs as follows,

$$\begin{aligned} U_{\mathrm{P}} &= v_{\mathrm{rD}} v_{\mathrm{sD}} + v_{\mathrm{rQ}} v_{\mathrm{sQ}} \\ U_{\mathrm{Q}} &= v_{\mathrm{rD}} v_{\mathrm{sQ}} - v_{\mathrm{rQ}} v_{\mathrm{sD}}. \end{aligned} \tag{15}$$

To eliminate the coupling terms, the new control inputs can be designed by using (13) (14) and (15) as follows,

$$\begin{aligned} U_{\mathrm{P}} =& -V'_{\mathrm{p}} - \underbrace{\frac{2\sigma L_{\mathrm{s}} L_{\mathrm{r}}}{3L_{\mathrm{m}}}(\frac{\omega_{\mathrm{m}}}{\sigma} + \omega_{\mathrm{r}})}_{K_{\mathrm{Qs}}} Q_{\mathrm{s}} - \frac{L_{\mathrm{r}}}{L_{\mathrm{m}}}|v_{\mathrm{s}}|^2 \\ & \underbrace{+R_{\mathrm{r}}(v_{\mathrm{sD}} i_{\mathrm{rD}} + v_{\mathrm{sQ}} i_{\mathrm{rQ}}) + \omega_{\mathrm{m}} L_{\mathrm{r}}(v_{\mathrm{sD}} i_{\mathrm{rQ}} - v_{\mathrm{sQ}} i_{\mathrm{rD}})}_{\text{compensation term } \mathrm{C_d}}, \end{aligned} \tag{16}$$

$$\begin{aligned} U_{\mathrm{Q}} =& -V'_{\mathrm{q}} + \underbrace{\frac{2\sigma L_{\mathrm{s}} L_{\mathrm{r}}}{3L_{\mathrm{m}}}(\frac{\omega_{\mathrm{m}}}{\sigma} + \omega_{\mathrm{r}})}_{K_{\mathrm{Ps}}} P_{\mathrm{s}} \\ & + \underbrace{R_{\mathrm{r}}(v_{\mathrm{sQ}} i_{\mathrm{rD}} - v_{\mathrm{sD}} i_{\mathrm{rQ}}) + \omega_{\mathrm{m}} L_{\mathrm{r}}(v_{\mathrm{sQ}} i_{\mathrm{rQ}} + v_{\mathrm{sD}} i_{\mathrm{rD}})}_{\text{compensation term } \mathrm{C_q}}, \end{aligned} \tag{17}$$

where V'_{p} and V'_{q} are the new control inputs, K_{Ps} and K_{Qs} are the power compensation parameters,C_q and C_d are the coupling compensation terms. In this paper, we choose a PI controller to produce V'_{p} and V'_{q} as,

$$V'_{\mathrm{p}} = K_{\mathrm{p,P}}(P^*_{\mathrm{s}} - P_{\mathrm{s}}) + K_{i,P}\int(P^* - P)dt \tag{18}$$

$$V'_{\mathrm{q}} = K_{\mathrm{p,Q}}(Q^*_{\mathrm{s}} - Q_{\mathrm{s}}) + K_{i,Q}\int(Q^* - Q)dt, \tag{19}$$

where P^* and Q^* are the references of active and reactive powers, respectively, and $K_{\mathrm{p,P}}$, $K_{\mathrm{i,P}}$, $K_{\mathrm{p,Q}}$, $K_{\mathrm{i,Q}}$ are the control parameters. Finally, by using the inversion of (15), the controlled RSC terminal voltage signal in DQ reference frame can be calculated as,

$$v_{\mathrm{rD}} = \frac{v_{\mathrm{sD}} U_P + v_{\mathrm{sQ}} U_{\mathrm{Q}}}{|v_{\mathrm{s}}|^2} \tag{20}$$

$$v_{\mathrm{rQ}} = \frac{v_{\mathrm{sQ}} U_P - v_{\mathrm{sD}} U_{\mathrm{Q}}}{|v_{\mathrm{s}}|^2}. \tag{21}$$

The controller for active and reactive powers can be constructed as shown in Fig. 3.

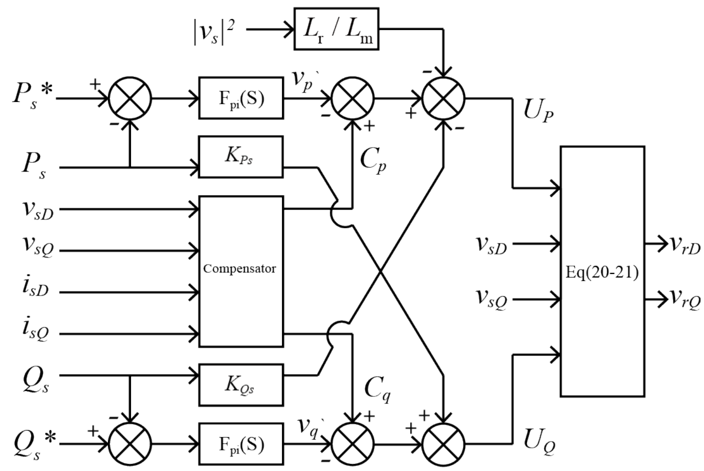

Fig. 3. Proposed control strategy by using the PI controllers.

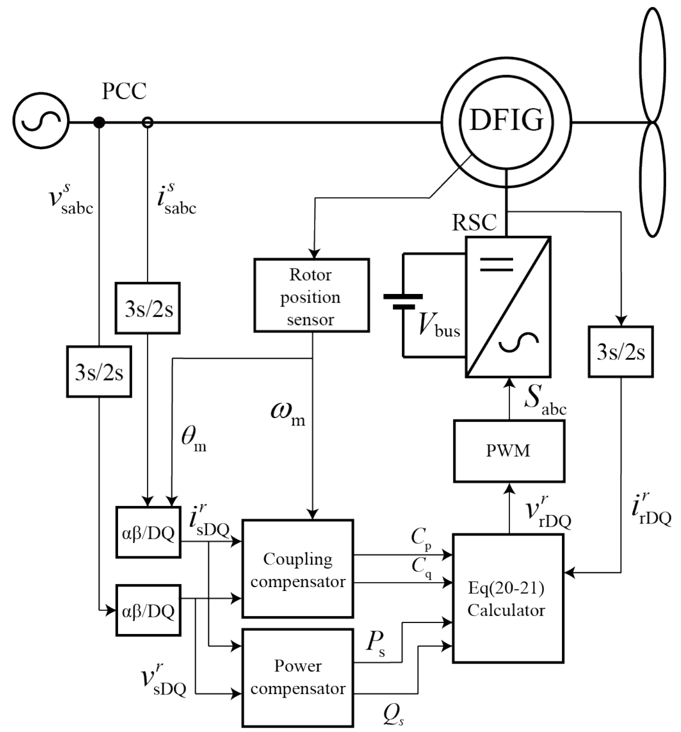

Fig. 4. Scheme diagram of the proposed VM-DPC control system for DFIGs.

TABLE I
PARAMETERS OF THE SIMULATED SYSTEM

Rated power	2 MW
Line-to line voltage (rms)	690 V
Stator frequency f	50 Hz
Stator-to-rotor ratio	3
R_s (ohm)	0.0026
R_r (ohm)	0.0029
L_s (mH)	2.6
L_r (mH)	2.6
L_m (mH)	2.5
Pole pairs p	2
$K_{p,P}$	0.15
$K_{i,P}$	0.5
$K_{p,Q}$	0.15
$K_{i,P}$	0.5
K_{opt}	29645

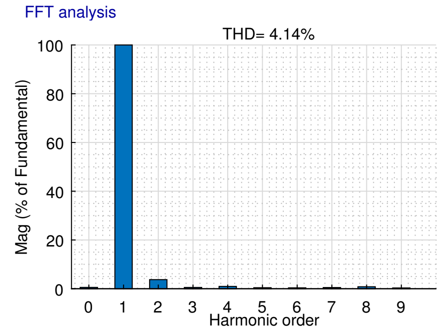

Fig. 6. Stator current spectrum of VM-DPC under steady-state (THD=4.14%).

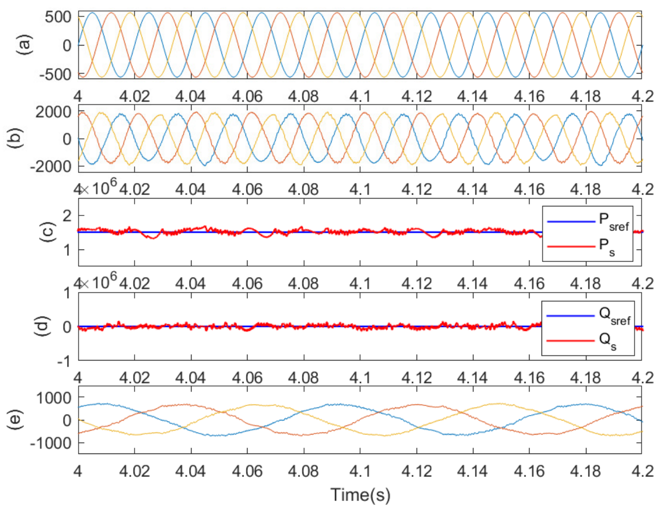

Fig. 5. Simulation result of the DFIG under steady-state during 4.0 s-4.2 s at 120 rad/s. (a) Stator voltage (V), (b) stator current (A), (c) stator active power (W), (d) stator reactive power (W), (e) rotor current (A).

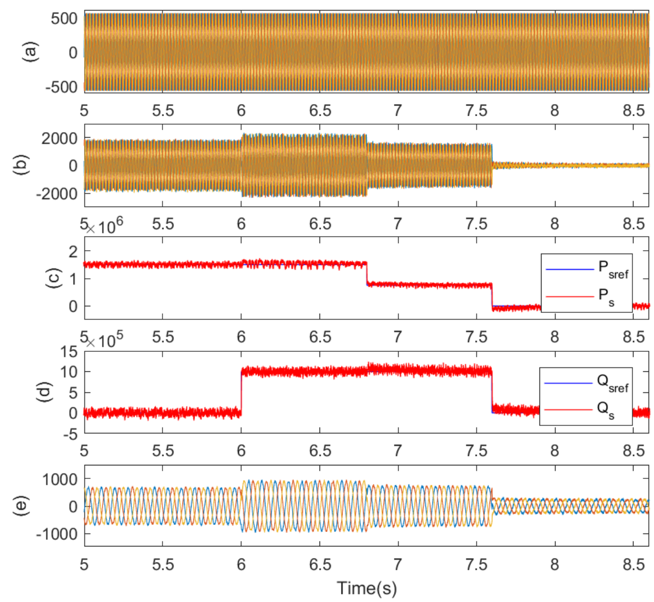

Fig. 7. Transient response of the VM-DPC strategy during 6.0 s-7.6 s at 120 rad/s rotor speed. (a) Stator voltage(V), (b)stator current (A), (c) stator active power (W), (d) stator reactive power (W), (e) rotor current (A).

IV. SIMULATION RESULTS

The proposed voltage modulated DPC for DFIG was carried out using MATLAB/Simulink. Fig. 4 shows the scheme of the implemented system in which the behavior of a specific 2 MW DFIG is studied. The rotor side converter of the generator is connected with a dc power supply, the dc-link is set to 1150 V. The speed of the machine is controlled externally to 120 rad/s. The parameters of the DFIG and controller are shown in Table I. The quality of the steady state behavior is shown in Fig. 5. A comparative simulations involving VM-DPC based system and a traditional VOC based control system designed in [20] to verify the transient and steady-state performance of VM-DPC.

The steady-state behavior of the presented DPC strategy is shown in Fig. 5. The stator active power reference is set to 1.5 MW and reactive power reference is set to 0 MW. The frequency 2-level PWM generator is set to 4-kHz. The VM-DPC with sinusoidal PWM has the output stator current THD of 4.1% which is less than 5% as commonly required for grid operation as shown in Fig. 6. The dynamic response of proposed VM-DPC and VOC were studied and compared as shown in Fig. 7 and Fig. 8. A severe stator active and reactive power variations will be demanded for that purpose. The control strategies will ensure that the machine responds to the demand in a quick and safe manner. The selected power variations are 7.5 kW and 5 kVAR, and they were accomplished at different instants. The first and the second power variations will affect to only one of the power references, while the third will demand a simultaneous active and reactive power variation. the step change of stator active power or reactive power does not affect the other, and there is no overshoot of either active and reactive powers. Nonetheless, because of the the elimination of slow dynamic loops such as PLL and inner current loop, the proposed VM-DPC has a much faster step response speed than VOC. It also manifests excellent steady-state performance close to VOC as simulation results show. Thus, it can be concluded from the performance

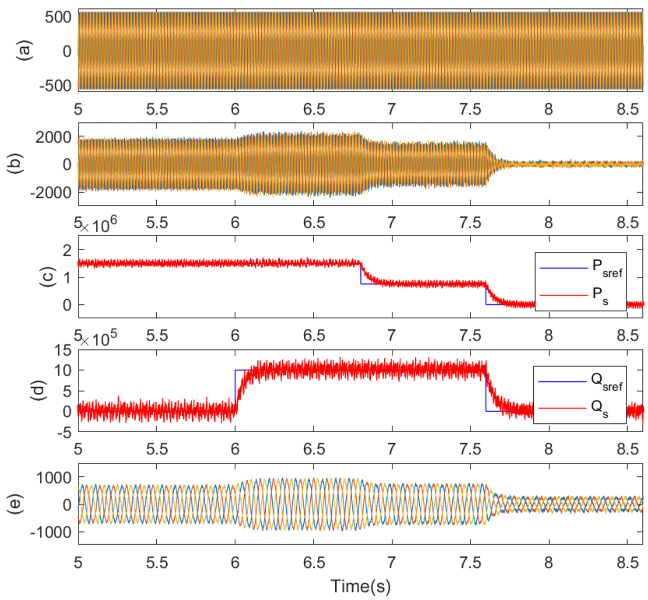

Fig. 8. Transient response of the VOC strategy during 6.0 s-7.6 s at 120rad/s rotor speed. (a) Stator voltage (V), (b) stator current (A), (c) stator active power (W),(d) stator reactive power (W), (e) rotor current (A).

comparison that the VM-DPC not only inherits excellent dynamic performance from VOC, but also has excellent steady state performance close to the VOC.

V. Conclusion

In this paper, an improved DPC control architecture called VM-DPC for the wind-turbine drived DFIG is proposed to control the stator active and reactive powers directly. The VM-DPC eliminates the slow-dynamic loops which have been widely adopted in VOC based strategies, thus it obtains not only fast convergence of the instantaneous active and reactive powers but also improves the steady-state performance. The proposed method was verified based on MATLAB/Simulink. The simulation results show that the proposed method has significantly improve the transient performance of DFIG and the THD of output stator current is much less than the requirement.

References

[1] Q. Wu and Y. Sun, *Modeling and Modern Control of Wind Power*. John Wiley & Sons, 2018.

[2] J. Hu, Y. He, L. Xu, and B. W. Williams, "Improved control of DFIG systems during network unbalance using PI-R current regulators," *IEEE Trans. Ind. Electron.*, vol. 56, no. 2, pp. 439–451, 2009.

[3] J. Hu, H. Nian, B. Hu, Y. He, and Z. Q. Zhu, "Direct active and reactive power regulation of DFIG using sliding-mode control approach," *IEEE Trans. Energy Convers.*, vol. 25, no. 4, pp. 1028–1039, 2010.

[4] H. Nian, S. Member, P. Cheng, and Z. Q. Zhu, "Coordinated direct power control of DFIG system without phase locked loop under unbalanced grid voltage conditions," *IEEE Trans. Power Electron.*, vol. 8993, no. c, pp. 1–14, 2015.

[5] P. Xiong and D. Sun, "Backstepping-based DPC strategy of a wind turbine-driven DFIG under normal and harmonic grid voltage," *IEEE Trans. Power Electron.*, vol. 31, no. 6, pp. 4216–4225, 2016.

[6] P. Zhou, Y. He, and D. Sun, "Improved direct power control of a DFIG-based wind turbine during network unbalance," *IEEE Trans. Power Electron.*, vol. 24, no. 11, pp. 2465–2474, 2009.

[7] X. Lie and P. Cartwright, "Direct active and reactive power control of DFIG for wind energy generation," *IEEE Trans. Energy Convers.*, vol. 21, no. 3, pp. 750–758, 2006.

[8] L. Shang and J. Hu, "Sliding-mode-based direct power control of grid-connected wind-turbine-driven doubly fed induction generators under unbalanced grid voltage conditions," *IEEE Trans. Energy Convers.*, vol. 27, no. 2, pp. 362–373, 2012.

[9] H. Nian, Y. Song, P. Zhou, and Y. He, "Improved direct power control of a wind turbine driven doubly fed induction generator during transient grid voltage unbalance," *IEEE Trans. Energy Convers*, vol. 26, no. 3, pp. 976–986, 2011.

[10] C. Liu, F. Blaabjerg, W. Chen, and D. Xu, "Stator current harmonic control with resonant controller for doubly fed induction generator," *IEEE Trans. Power Electron.*, vol. 27, no. 7, pp. 3207–3220, 2012.

[11] H. Nian and Y. Song, "Direct power control of doubly fed induction generator under distorted grid voltage," *IEEE Trans. Power Electron.*, vol. 29, no. 2, pp. 894–905, 2014.

[12] G. Abad and M. Angel, "Direct power control of the doubly fed induction machine with reduced power ripple at low constant switching frequency," *IEEE Trans. Energy Convers.*, vol. 23, no. 2, pp. 570–580, 2008.

[13] J.-P. G. Abdelouahab Bouafia, "Predictive direct power control of three-phase pulsewidth modulation (PWM) rectifier using space-vector modulation (SVM)," *IEEE Trans. Power Electron.*, vol. 25, no. 1, pp. 228–236, 2010.

[14] G. Abad, M. Á. Rodríguez, and J. Poza, "Three-level NPC converter-based predictive direct power control of the doubly fed induction machine at low constant switching frequency," *IEEE Trans. Ind. Electron.*, vol. 55, no. 12, pp. 4417–4429, 2008.

[15] L. Li and H. Nian, "Direct power control of DFIG system without phase-locked loop under unbalanced and harmonically distorted voltage," *IEEE Trans. Energy Convers.*, vol. 33, no. 1, pp. 395–405, 2018.

[16] Y. Gui, C. Kim, and C. C. Chung, "Grid voltage modulated direct power control for grid connected voltage source inverters," in *Amer. Control Conf.*, pp. 2078–2084, 2017.

[17] Y. Gui, C. Kim, C. C. Chung, J. M. Guerrero, Y. Guan, and J. C. Vasquez, "Improved direct power control for grid-connected voltage source converters," *IEEE Trans. Ind. Electron.*, vol. 65, no. 10, pp. 8041–8051, 2018.

[18] Y. Gui, M. Li, J. Lu, S. Golestan, J. M. Guerrero, and J. C. Vasquez, "A voltage modulated DPC approach for three-phase PWM rectifie," *IEEE Trans. Ind. Electron.*, vol. 65, no. 10, pp. 7612–7619, 2018.

[19] Y. Gui, B. Wei, M. Li, J. M. Guerrero, and J. C. Vasquez, "Passivity-based coordinated control for islanded AC microgrid," *Appl. Energy*, vol. 229, pp. 551–561, 2018.

[20] H. Abu-Rub, M. Malinowski, and K. Al-Haddad, *Properties and Control of a Doubly Fed Induction Machine*. IEEE, 2014.